Structural and Electron Paramagnetic Resonance Studies of the Square Pyramidal to Trigonal Bipyramidal Distortion of Vanadyl Complexes Containing Sterically Crowded Schiff Base Ligands

Charles R. Cornman*, Katherine M. Geiser-Bush, Stephen P. Rowley, and Paul D. Boyle

Department of Chemistry, North Carolina State University, Raleigh, North Carolina 27695-8204

Received July 10, 1997[⊗]

[*N*,*N*′-Ethylenebis(*o*-(*tert*-butyl-*p*-methylsalicylaldiminato)]oxovanadium(IV) (**1**), [*N*,*N*′-propanediylbis(*o*-(*tert*-butyl-*p*-methylsalicylaldiminato)]oxovanadium(IV) (**2**), bis(*N*-methylsalicylaldiminato)oxovanadium(IV) (**3**), bis(*N*-isopropyl-*o*-methylsalicylaldiminato)oxovanadium(IV) (**4**), and, bis(*N*-methyl-*o*-(*tert*-butyl-*p*-methylsalicylaldiminato)-oxovanadium(IV) (**5**) were prepared and characterized by X-ray crystallography and EPR spectroscopy. Complexes **1** and **2** are best described as square pyramids, while complexes **3**−**5** are distorted trigonal bipyramids, demonstrating that oxovanadium(IV) complexes can readily adopt a trigonal bipyramidal geometry. All five compounds give nearly the same parallel hyperfine coupling constant (A_z) regardless of the fact that the geometry about the vanadium changes from square pyramidal to trigonal bipyramidal. Crystal data for **1**: space group $P\bar{1}$, $a = 7.9382(3)$ Å, $b = 12.6749(7)$ Å, $c = 13.8353(7)$ Å, $\alpha = 109.608(5)°$, $\beta = 96.552(5)°$, $\gamma = 96.589(5)°$, $Z = 2$. Crystal data for **2**: space group $I4_1/a$, $a = 16.1895(6)$ Å, $b = 16.1895(6)$ Å, $c = 41.117(3)$ Å, $Z = 16$. Crystal data for **3**: space group $C2/c$, $a = 18.8230(17)$ Å, $b = 7.5118(5)$ Å, $c = 11.7460(10)$ Å, $\beta = 112.229(7)°$, $Z = 4$. Crystal data for **4**: space group $P2_1/c$, $a = 9.7086(6)$ Å, $b = 11.4554(7)$ Å, $c = 20.866(2)$ Å, $\beta = 103.943(6)°$, $Z = 4$. Crystal data for **5**: space group *Pbca*, $a = 10.667(3)$ Å, $b = 25.549(5)$ Å, $c = 18.322(4)$ Å, $Z = 8$.

Introduction

The coordination chemistry of vanadium has recently become of great interest due to the presence of vanadium in enzymatic systems and the ability of vanadium complexes to elicit the effects of insulin in diabetic animals.[1,2] Much of the biochemistry of vanadium is centered around the ability of vanadate ($H_2V^VO_4^{2-}$) to adopt a four-coordinate, tetrahedral geometry and a five-coordinate, trigonal bipyramidal (tbp) geometry; the tetrahedral ions are analogues of the phosphate anion, while the tbp complexes are analogues of the transition state for phosphoester hydrolysis.[3] We have been interested in the vanadium-based inhibition of protein tyrosine phosphatases (PTPs), especially with regard to the potential role of vanadium−PTP adducts in the observed insulin-like effects of vanadium.[4−7] Several lines of evidence suggest that vanadium(IV), as well as vanadium(V), may be responsible for this observation. First, a vanadium(V)/vanadium(IV) equilibrium is established in the reducing environment of living cells.[8,9] Second, a distinct vanadium(IV)-dependent (and vanadium(V)-independent) system for activating insulin-like effects has recently been reported.[9] Third, we have previously shown by EPR spectroscopy that vanadium(IV) ion forms adducts of the active site polypeptide of PTP-1B in which the vanadium coordinates to either the cysteine thiolate or histidine imidazole.[10] Protein crystallography of two V−PTP complexes indicates that vanadium forms a tbp adduct at the active site of the enzyme, as depicted in Scheme 1.[11,12] The oxidation state of the vanadium cannot be determined from the protein crystallography; however, the general opinion is that the vanadium is in the +5 oxidation state. As discussed by Carrano, vanadium(V) typically forms square pyramidal (sq pyr), five-coordinate complexes or octahedral, six-coordinate complexes except when significant steric constraints, such as those provided by a protein, are present.[13]

Scheme 1

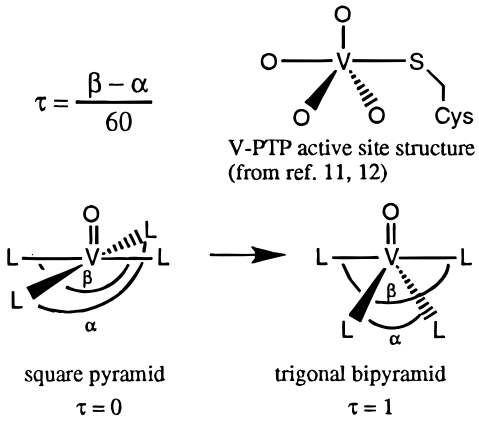

The structural chemistry of small vanadium(IV) molecules is well-established, and, as with vanadium(V), the preponderance of five-coordinate vanadium(IV) complexes adopt a sq pyr or distorted sq pyr geometry. To quantitatively compare these

[⊗] Abstract published in *Advance ACS Abstracts,* December 1, 1997.

(1) *Vanadium in Biological Systems*; Chasteen, N. D., Ed.; Kluwer Academic Publishers: Dordrecht, The Netherlands, 1990.
(2) *Vanadium and its role in life*; Sigel, H., Sigel, A., Eds.; Marcel Decker: New York, 1995; Vol. 31.
(3) Crans, D. C. *Comments Inorg. Chem.* **1994**, *16*, 35−76.
(4) Shechter, Y.; Karlish, S. J. D. *Nature* **1980**, *284*, 556−558.
(5) Dubyak, G. R.; Kleinzeller, A. *J. Biol. Chem.* **1980**, *255*, 5306−5312.
(6) Yuen, V. G.; Orvig, C.; McNeill, J. H. *Can. J. Physiol. Pharmacol.* **1993**, *71*, 263−269.
(7) Shisheva, A.; Shechter, Y. *J. Biol. Chem.* **1993**, *268*, 6463−6469.
(8) Degani, H.; Gochin, M.; Karlish, S. J. D.; Shechter, Y. *Biochemistry* **1981**, *20*, 5795−5799.
(9) Li, J.; Elberg, G.; Crans, D. C.; Shechter, Y. *Biochemistry* **1996**, *35*, 8314−8318.
(10) Cornman, C. R.; Zovinka, E. P.; Meixner, M. H. *Inorg. Chem.* **1995**, *34*, 5099−5100.
(11) Zhang, M.; Zhou, M.; Van Etten, R. L.; Stauffacher, C. V. *Biochemistry* **1997**, *36*, 15−23.
(12) Denu, J. M.; Lohse, D. L.; Vijayalakshmi, J.; Saper, M.; Dixon, J. E. *Proc. Natl. Acad. Sci. U.S.A.* **1996**, *93*, 2493−2498.
(13) Morky, L. M.; Carrano, C. J. *Inorg. Chem.* **1993**, *32*, 6119−6121.

S0020-1669(97)00868-9 CCC: $14.00

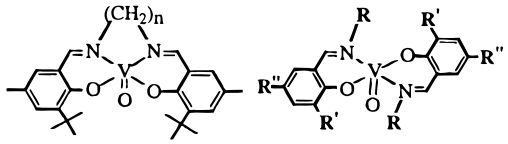

complex	n	R	R'	R"
1	2			
2	3			
3		Me	H	H
4		*i*-Pr	Me	H
5		Me	*t*-Bu	Me

Figure 1. Vanadyl complexes studied.

structures in terms of their relative geometries about the vanadium atom, we have used the angular structural parameter, τ, which is defined in Scheme 1.[14] For purely square pyramidal complexes τ is zero. Moving two trans ligands out of the equatorial square plane results in a distortion toward a "trigonal bipyramid" for which τ approaches 1 ($\tau = 1$ for a perfect trigonal bipyramid). In this paper, we use the term "trigonal bipyramid" to describe the molecular geometry, not the molecular symmetry which would be D_{3h} for a true trigonal bipyramid. It should be noted that the symmetry change shown in Scheme 1 is C_{4v} to C_{2v} if all equatorial ligands are equivalent. For our purposes, we will describe complexes with $0 \leq \tau \leq 0.5$ as distorted square pyramids, while complexes with $0.5 < \tau \leq 1$ will be described as distorted trigonal bipyramids. A search of the Cambridge Structural Database for monomeric five-coordinate vanadyl complexes with O/N donors yields 56 structures.[15] Of these, only $V^{IV}O(quinolinol)_2$ is a distorted tbp ($\tau = 0.56$).[16] The paucity of tbp structures for vanadium(IV) suggests that there are electronic and/or steric requirements that preclude the formation of the tbp geometry. To probe these requirements, we have prepared a series of vanadyl complexes (the term vanadyl is used for $V^{IV}O^{2+}$) in which the heteroatom donors remain constant but the geometry about the metal varies. Herein we report the synthesis and characterization of five pentacoordinate vanadyl complexes (Figure 1), three of which are best described as having distorted tbp geometries. The EPR spectra of these complexes are also reported, and the relationship among structure, bonding, and spectral parameters is discussed.

Experimental Section

Synthesis. *o-tert*-Butyl-*p*-methylsalicylaldehyde[17] and vanadyl acetate[18] were prepared by literature methods. Acetonitrile was dried by distillation from CaH_2 under dinitrogen. Schiff base ligands were prepared by refluxing a mixture of salicylaldehyde (or substituted salicylaldehyde) and the appropriate amine (or amine hydrochloride and KOH) in ethanol for 20 min. The ligands crystallized upon cooling and/or evaporation of the solvent. Ligand identity was verified by ^{1}H NMR and IR (not shown). All other materials were reagent grade and used as received from commercial sources.

[*N*,*N*′-Ethylenebis(*o*-(*tert*-butyl-*p*-methylsalicylaldiminato)]oxovanadium(IV) (**1**) was prepared by a template reaction adapted from the procedure of Carrano[19] in which *o-tert*-butyl-*p*-methylsalicylaldehyde (0.25 g, 1.3 mmol), ethylenediamine (0.044 mL, 0.65 mmol), and vanadium tris(acetylacetonate) (0.23 g, 0.65 mmol) were refluxed in absolute ethanol for about an hour under an aerobic atmosphere. After the solution cooled, the bright green solid was collected by filtration. Yield: 0.18 g, 58%. Dark green diffraction quality crystals (as needles) were obtained by slow evaporation of an acetone solution. IR: ν(V═O), 988 cm^{-1}. Anal. Found (calcd): %C, 65.55 (65.95); %H, 7.17 (7.24); %N, 5.93 (5.92).

[*N*,*N*′-Propanediylbis(*o-tert*-butyl-*p*-methylsalicylaldiminato)]oxovanadium(IV) (**2**) was prepared under a dinitrogen atmosphere using standard techniques. The ligand (0.20 g, 0.48 mmol) and vanadyl acetate (0.073 g, 0.40 mmol) were refluxed in dry acetonitrile for 24 h. The olive green solution was concentrated under vacuum to yield a green precipitate that was collected by filtration and recrystallized from hot acetonitrile. Yield: 0.19 g, 83%. Dark green diffraction quality crystals of complex **2** were obtained from slow evaporation of a toluene solution. IR: ν(V═O), 984 cm^{-1}. Anal. Found (calcd): %C, 66.55 (66.52); %H, 7.66 (7.44); %N, 5.65 (5.75).

Bis(*N*-methylsalicylaldiminato)oxovanadium(IV) (**3**) was prepared following the procedures of Floriani and co-workers.[20] The ligand (1.0 g, 7.4 mmol) was dissolved in ethanol and added to an aqueous solution of vanadyl sulfate (0.60 g, 3.7 mmol). Sodium acetate (1.3 g, 15 mmol) was then added as an aqueous solution. The reaction mixture was refluxed for 20 min. The fine brown powder was filtered after 2 h and washed in water, ethanol, and diethyl ether. Yield: 0.53 g, 43%. Diffraction quality crystals of complex **3** (brown blocks) were obtained by slow cooling of a hot acetonitrile solution. IR: ν(V═O), 980 cm^{-1}. Anal. Found (calcd): %C, 57.22 (57.32); %H, 4.90 (4.81); %N, 8.40 (8.36).

Bis(*N*-isopropyl-*o*-methylsalicylaldiminato)oxovanadium(IV) (**4**) was prepared in a manner analogous to complex **3**. Yield: 37%. Diffraction quality crystals of complex **4** (brown blocks) were obtained by slow cooling of an acetonitrile solution. IR: ν(V═O), 976 cm^{-1}. Anal. Found (calcd): %C, 62.66 (63.00); %H, 6.69 (6.73); %N, 6.59 (6.68).

Bis(*N*-methyl-*o-tert*-butyl-*p*-methylsalicylaldiminato)oxovanadium-(IV) (**5**) was prepared similarly to complexes **3** and **4**. The ligand (57 mg, 0.28 mmol) and sodium acetate (25 mg, 0.31 mmol) were dissolved in methanol. An aqueous solution of vanadyl sulfate (42 mg, 0.14 mmol) was added after a few minutes of stirring, and the reaction mixture was refluxed for 3 h. The solution was allowed to cool to room temperature and then was kept at 0 °C for 24 h. The resulting gold precipitate was then filtered and recrystallized from hot acetonitrile. Yield: 0.038g, 58%. IR: ν(V═O), 968 cm^{-1}. Anal. Found (calcd): %C, 65.33 (65.67); %H, 7.58 (7.63); %N, 8.73 (5.89). Complex **5** can also be prepared by refluxing the ligand (0.10 g, 0.51 mmol) with vanadyl acetate (0.047 g, 0.25 mmol) in acetonitrile under a dinitrogen atmosphere for 24 h. The olive green precipitate was collected by filtration and washed several times with acetonitrile and gave the identical ν(V═O) and EPR signal as the above procedure. Yield: 0.063 g, 52%. Diffraction quality crystals of complex **5** (green cubes) were obtained by slow diffusion of ethanol into a toluene solution of complex **5** from this second procedure under an inert atmosphere. Large-scale purification from this second procedure did not yield analytically pure complex.

X-ray Data Collection. Crystallographic data acquisition parameters for all five compounds are given in Table 1. The unit cell dimensions of all crystals were determined by a symmetry constrained fit of 24 well-centered reflections and their Friedel pairs.

For complex **1**, one hemisphere of data was collected using the $\theta/2\theta$ scan mode. For complex **2**, one-sixteenth of a sphere was collected using the ω scan mode. Some redundant data (approximately 400 reflections) were collected to check data quality ($R_{merg} = 0.02$). For complex **3**, a unique quadrant of data was collected using the ω scan mode in a non-bisecting geometry. The adoption of a non-bisecting scan mode was accomplished by offsetting ψ by 20.00 for each data point collected. This was done to minimize the interaction of the goniometer head with the cold stream. A unique quadrant of data was collected for complex **4** using the $\theta/2\theta$ scan mode. An octant of data was collected for complex **5** using the ω scan mode and a bisecting geometry (83 redundant reflections were collected due to instrumental difficulties). The data were collected in a nonstandard setting and transformed to a standard setting before data reduction.

(14) Addison, A. W.; Rao, T. N.; Reedijk, J.; van Rijn, J.; Verschoor, G. C. *J. Chem. Soc., Dalton Trans.* **1984**, 1349−1356.
(15) Allen, F. H.; Kennard, O. *Chem. Des. Autom. News* **1993**, *8*, 31−37.
(16) Shiro, M.; Fernando, Q. *Anal. Chem.* **1971**, *43*, 1222−1230.
(17) Casiraghi, G.; Casnati, G.; Puglia, G.; Sartori, G.; Terenghi, G. *J. Chem. Soc., Perkin Trans. 1* **1980**, 1862−1865.
(18) Paul, R. C.; Bhatia, S.; Kumar, A. In *Inorganic Synthesis*; Cotton, F. A., Ed.; McGraw-Hill: New York, 1972; Vol. 13, pp 181−183.
(19) Bonadies, J. A.; Carrano, C. J. *J. Am. Chem. Soc.* **1986**, *108*, 4088−4095.
(20) Pasquali, M.; Marchetti, F.; Floriani, C. *J. Chem. Soc., Dalton Trans.* **1977**, 139−144.

Table 1. Crystallographic Data for Complexes **1**−**5**

	1	**2**	**3**	**4**	**5**
formula	$C_{26}H_{34}N_2O_3V$	$C_{27}H_{36}N_2O_3V$	$C_{16}H_{16}N_2O_3V$	$C_{22}H_{28}N_2O_3V$	$C_{26}H_{36}N_2O_3V$
fw	473.51	487.53	335.26	419.41	475.52
temp	ambient	ambient	−110 °C	ambient	ambient
space group	$P\bar{1}$	$I4_1/a$	$C2/c$	$P2_1/c$	$Pbca$
a (Å)	7.9382(3)	16.1895(6)	18.8230(17)	9.7086(6)	10.667(3)
b (Å)	12.6749(7)	16.1895(6)	7.5118(5)	11.4554(7)	25.549(5)
c (Å)	13.8353(7)	41.117(3)	11.7460(10)	20.866(2)	18.322(4)
α (deg)	109.608(5)	90	90	90	90
β (deg)	96.522(5)	90	112.229(7)	103.943(6)	90
γ (deg)	96.589(5)	90	90	90	90
V (Å^3)	1285.35(11)	10776.8(9)	1537.4(2)	2252.2(3)	4993(2)
ρ_{calc} (g cm^{-3})	1.223	1.202	1.448	1.237	1.265
Z	2	16	4	4	8
λ (Mo Kα)	0.710 73	0.710 73	0.710 73	0.710 73	0.710 73
μ (cm^{-1})	3.99	3.82	6.4	4.5	4.10
R^a	0.039	0.055	0.038	0.037	0.054
$R_w{}^b$	0.058	0.063	0.047	0.045	0.056

^{a} $R = \sum(F_o - F_c)/\sum(F_o)$. ^{b} $R_w = [\sum(w(F_o - F_c)^2)/\sum(wF_o^2)]^{1/2}$.

For all crystals, three standard reflections were measured every 4800 s of X-ray exposure time. Decomposition was not observed. Scaling the data was accomplished using a five-point smoothed-curve routine fitted to the intensity check reflections. Intensity data were corrected for Lorentz and polarization effects. An empirical absorption correction derived from ψ-scan data was also applied during data reduction for complexes **1** and **2**. The empirical absorption was not applied for complex **3** or **4** due to the small absorption coefficient as well as the lack of dependence on φ of the intensity of a high χ reflection. No absorption correction was applied for **5** because the ψ-scan data indicated no dependence of the intensity on φ.

Structure Solution and Refinement. The data for complexes **1**−**5** were reduced using routines from the NRCVAX set of programs.[21] The structures were solved using SIR92.[22] All non-hydrogen atoms were recovered from the initial E-maps. For complexes **1**, **2**, and **5** the hydrogen atoms were initially placed at idealized positions. The carbon−hydrogen distances were set to 0.96 Å and the isotropic displacements, U(H), were set according to the expression $U(H) = U(C) + 0.01$. In complexes **3** and **4**, subsequent difference Fourier maps yielded peaks suggestive of hydrogen atom positions, and these were entered as such. The atomic position and anisotropic displacement parameters refined smoothly using the NRCVAX LSTSQ routine. The calculated structure factors were fit to the data using full-matrix least-squares based on F. All non-hydrogen atoms were refined anisotropically. The hydrogen atoms in complexes **1** and **2** were included in the structure factor calculations but not refined. In complexes **3** and **4**, the hydrogen atom positional and isotropic displacement parameters were allowed to refine. The orientation of the methyl groups of complex **5** were refined using a constrained group refinement. After the refinement of the methyl groups' orientations converged, all hydrogen atoms were allowed to ride on the parent carbon atom. The hydrogen positional and displacement parameters were updated after every other cycle of least-squares. For all five structures, the calculated structure factors included corrections for anomalous dispersion from the usual tabulation.[23] A secondary extinction correction was not included in the final cycles of refinement for complexes **1**, **2**, and **5**. Extinction refinement in the intermediate least-squares cycles gave a value which was zero within 1 σ. Secondary extinction corrections were attempted for complexes **3** and **4** but were disregarded in the final refinements because the extinction coefficients obtained were physically meaningless.

Spectroscopy. Infrared spectra were obtained on KBr pellets using a Mattson Polaris spectrometer. EPR spectra were obtained on an IBM ER200D instrument operating at X-band (≈9.45 GHz). Microwave frequency was measured with a Hewlett-Packard 5350B frequency counter, and the field at $g = 2.0037$ was calibrated with DPPH. The field linearity (<1 G over 1400 G) was confirmed by comparison of the parallel transitions for vanadyl sulfate (1:1 H_2O:glycerin; pH 2 adjusted with HCl) with those based on the literature ($g_z = 1.933$, $A_z = 182.6 \times 10^{-4}$ cm^{-1}, $g_{x,y} = 1.978$, $A_{x,y} = 70.7 \times 10^{-4}$ cm^{-1}).[24] All spectra were collected on toluene solutions at 150 K using a quartz insert and an IBM ER4111VT temperature controller. Microwave power was 2−20 mW and field modulation was 5 G_{pp}. Analog EPR data were digitized using EPRWare.[25] Spectral parameters were fit using the program SIMPOW using coincident **A** and **g** tensors.[26,27] Non-coincident **A** and **g** tensors had little effect on the quality of the fit. The g- and A-values reported in Table 4 represent the average of three independent measurements. UV−vis spectra between 200 and 1100 nm were collected on CH_2Cl_2 solutions of complexes **1**−**5** using a Shimadzu UV 1601 instrument.

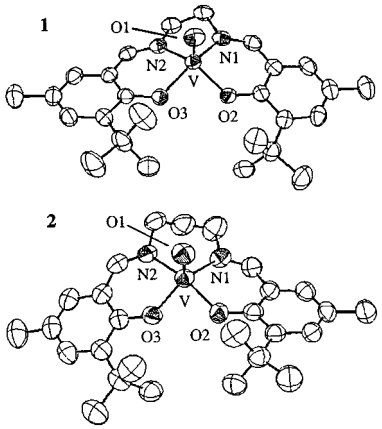

Figure 2. ORTEP diagrams (50% probability) of complexes **1** and **2**.

Results

Description of Structures. Structural diagrams of complexes **1** and **2** are presented in Figure 2. Structural diagrams of complexes **3** and **4** are presented in Figure 3. The structural diagram of complex **5** is presented in Figure 4. Selected bond distances and angles are given in Table 2. Complete geometric information and numbering schemes are given in the Supporting Information.

(21) Gabe, E. J.; Le Page, Y.; Charland, J.-P.; Lee, F. L.; White, P. S. *J. Appl. Crystallogr.* **1989**, *22*, 384−387.
(22) Altomare, A.; Burla, M. C.; Camalli, G.; Cascarano, G.; Giacovazzo, C.; Gualiardi, A.; Polidori, G. *J. Appl. Crystallogr.* **1994**, *27*, 435−436.
(23) *International Tables for X-Ray Crystallography*; Ibers, J., Hamilton, W., Eds.; Kynoch Press: Birmingham, England, 1974; Vol. IV.
(24) Albanese, N. F.; Chasteen, N. D. *J. Phys. Chem.* **1978**, *82*, 910−914.
(25) Morse, P. D., II. *Biophys. J.* **1987**, *51*, 440a.
(26) Nilges, M. *Program SIMPOW*; Illinois ESR Research Center NIH Division of Research Resources Grant No. RR01811.
(27) Mattson, K. J.; Clarkson, R. B.; Belford, R. L. *11th International EPR Symposium, 30th Rocky Mountain Conference*, Denver, CO, 1988.

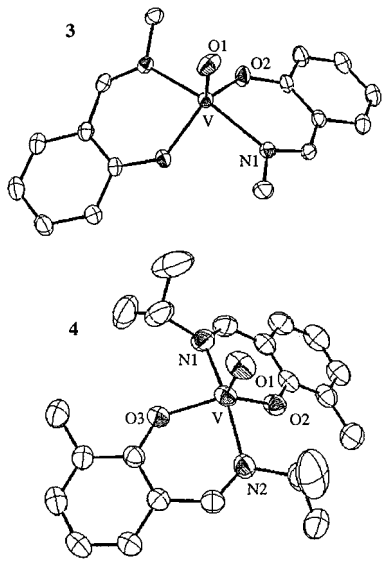

Figure 3. ORTEP diagrams (50% probability) of complexes **3** and **4**.

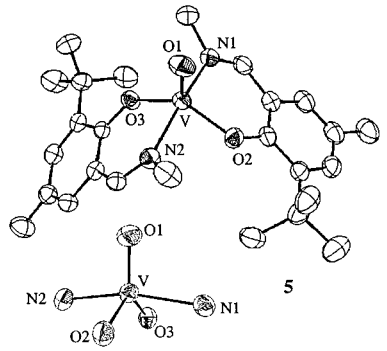

Figure 4. ORTEP diagram (50% probability) of complex **5**. Inset shows first coordination sphere to emphasize the tbp geometry.

Table 2. Selected Bond Lengths (Å) and Angles (deg) for Complexes **1**−**5**

	1	**2**	**3**[a]	**4**	**5**
V−O1	1.5913(13)	1.581(3)	1.590(4)	1.5988(18)	1.601(2)
V−O2	1.9226(12)	1.937(3)	1.893(3)	1.9117(16)	1.9005(17)
V−O3	1.9351(12)	1.954(3)		1.9149(16)	1.9027(16)
V−N1	2.0589(15)	2.095(3)	2.097(3)	2.096(2)	2.076(2)
V−N2	2.0710(15)	2.100(3)		2.098(2)	2.089(2)
O1−V−O2	113.18(7)	113.06(14)	115.2(1)	116.56(9)	117.66(9)
O1−V−O3	105.65(7)	103.65(14)		114.12(9)	118.36(9)
O1−V−N1	103.01(7)	97.97(14)	98.6(1)	97.77(10)	96.86(10)
O1−V−N2	111.08(7)	106.45(15)		98.07(10)	97.32(9)
O2−V−O3	88.44(5)	84.03(11)	129.6(2)	129.31(8)	123.99(8)
O2−V−N1	86.06(6)	85.45(13)	87.5(1)	86.84(8)	87.11(8)
O2−V−N2	135.21(6)	140.49(13)	85.2(1)	86.21(8)	87.34(8)
O3−V−N1	150.65(6)	158.26(13)		85.87(8)	86.07(7)
O3−V−N2	86.18(5)	86.90(13)		87.56(7)	86.19(7)
N1−V−N2	77.72(6)	89.21(14)	162.8(2)	164.17(9)	165.77(9)

[a] N2 and O3 refer to N′ and O′, respectively.

Similar to other VO(SALEN) [(*N*,*N*′-ethylenebis(salicylaldiminato)]oxovanadium(IV) type compounds,[28,29] complexes **1** and **2**, shown in Figure 2, are best described as distorted square pyramidal ($\tau = 0.26$ and 0.30, respectively) with the oxo ligands in axial positions and the donor atoms from the tetradentate ligands forming the equatorial plane. This places the two imine nitrogens and the two phenolate oxygens cis to one another. In complexes **1**, the $V-O_{oxo}$ bond distance of 1.591 Å is typical for five-coordinate vanadyl species. The average of the $V-O_{phenol}$ bond distances of 1.929 Å and the average of the $V-N_{imine}$ bond distances of 2.065 Å are in the range seen for many other vanadium−Schiff base complexes. Complex **2** has similar bond distances. The vanadium atoms sit 0.626 and 0.531 Å out of the best plane defined by N1−N2−O2−O3 in complexes **1** and **2**, respectively.

The structures of complexes **3** and **4** are shown in Figure 3. The geometry about the vanadium is best described as distorted trigonal bipyramidal for both complexes with $\tau = 0.55$ and 0.58, respectively. Complex **3** has crystallographically imposed C_2 symmetry, while complex **4** has approximate C_2 symmetry. The two bidentate Schiff base ligands in each complex are oriented trans to each other, with the oxo ligand in the "axial" position (axial direction defined as being along the highest rotation axis) and the imine nitrogens and the phenolate oxygens forming the "equatorial" plane. Once again the $V-O_{oxo}$, the $V-O_{phenol}$, and the $V-N_{imine}$ bond distances are typical, as in complexes **1** and **2**. For complex **3**, the β-angle N1−V−N′ (see Scheme 1) is 162.8° and the α-angle O2−V−O′ is 129.6°. Thus, the phenolate oxygens are displaced out of the "equatorial" plane away from the axial oxo ligand. The structural parameters of complex **4** are within 1.2% of those in complex **3**.

Complex **5**, shown in Figure 4, is even more distorted from square pyramidal toward trigonal bipyramidal ($\tau = 0.70$). Again, the first coordination sphere consists of "axial" oxo ligand and imine nitrogens and phenolate oxygen donors in the "equatorial" plane; however, in this structure, which has the bulkiest ligand substituents, the angles are the closest to a trigonal bipyramid for any monomeric vanadyl complex with N- and O-substitution.[15] The β-angle, 165.8°, is the most linear of those of complexes **1**−**5** (150.7° for **1**, 158.3° for **2**, 162.8° for **3**, and 164.2° for **4**). The α-angle of 124.0° more closely approaches that which is expected for a trigonal bipyramidal geometry than the other complexes (135.2° for **1**, 140.5° for **2**, 129.6° for **3**, and 129.3° for **4**). Vanadium−heteroatom bond distances in complex **5** are within 1% of the values for complexes **3** and **4**.

At this juncture, one should note that complexes **1** and **2** have approximate C_s symmetry. The symmetry plane, which bisects the O2−V−O3 angle, contains the *z*- and *x*-axis (or *y*-axis) and thus defines the molecular coordinate system. In complexes **1** and **2** the non-oxo ligands lie between the *x*- and *y*-axes. In contrast, complexes **3**−**5** have C_2 symmetry and the ligands lie in the *xz* or *yz* plane. For the discussion below, we have defined the *y*-axis in complexes **3**−**5** as the axis directed toward the nitrogen ligands. The difference between the C_s (complexes **1** and **2**) and the C_2 (complexes **3**−**5**) coordinate systems is a 45° rotation about the *z*-axis. This coordinate rotation has no effect on τ, which is still defined by the bond angles as shown in Scheme 1; however, the coordinate shift must be taken into account when the electronic structures of the complexes are considered.

Spectroscopy. The frequencies of the $V{=}O_{oxo}$ stretch for each compound are provided in the Experimental Section.[30,31] Electronic absorption data for complexes **1**−**5** are presented in Figure 5 and Table 3. Table 4 lists parameters derived from the EPR spectra of complexes **1**−**5**. EPR spectra are shown in Figure 6. All show rhombic EPR spectra with an increasing difference between the A_{xx} and A_{yy} values, which is predominantly due to a decrease in A_{xx}, as the geometry changes from square pyramidal to trigonal bipyramidal. The axis labels for

(28) Pasquali, M.; Marchetti, F.; Floriani, C.; Cesari, M. *Inorg. Chem.* **1980**, *19*, 1198−1202.
(29) Riley, P. E.; Pecoraro, V. L.; Carrano, C. J.; Bonadies, J. A.; Raymond, K. N. *Inorg. Chem.* **1986**, *25*, 154−160.
(30) Zamian, J. R.; Dockal, E. R. *Trans. Met. Chem.* **1996**, *21*, 370−376.
(31) Hamilton, D. E. *Inorg. Chem.* **1991**, *30*, 1670−1671.

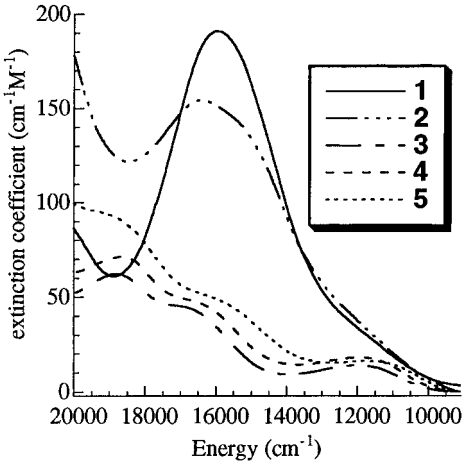

Figure 5. UV−vis spectra of complexes **1**−**5** in CH_2Cl_2.

the principle *g*- and *A*-values were assigned for complexes **3**−**5** by comparison to the single crystal EPR results for $V^{IV}O$-(quinolinol)$_2$.[32] The *g* and *A* axis labels for complexes **1** and **2** were arbitrarily chosen to coincide with those for complexes **3**−**5**. Best fits are provided in Figures S1 and S2 of the Supporting Information.

Discussion

The use of sterically large ligands to prepare energetically disfavored coordination geometries is a strategy that has been used extensively to study structure/property relationships. The goal of this work was to prepare five-coordinate oxovanadium(IV) complexes spanning the range of geometries from square pyramidal to trigonal bipyramidal. Despite the less-crowded environment of the trigonal bipyramidal geometry, most oxovanadium(IV) complexes form square pyramidal structures due to strong π-bonding from the axial oxo ligand and the use of tri- and tetradentate ligands that prefer a planar conformation for the donor set. In order to overcome this geometric preference, we have used (a) the sterically encumbered tetradentate bis-Schiff base ligands and (b) the sterically encumbered bidentate Schiff base ligands shown in Figure 1.

The two tetradentate ligands, which have the same donor atoms as the much used ligand SALEN, differ from each other only in the number of methylene groups (n = 2 or 3) that connect the salicylideneamine moieties. The *tert*-butyl substituents were added to increase the steric bulk within the equatorial plane and prevent the formation of oligomers that are common for vanadyl complexes of this type when the N,N-chelate forms a six-membered ring (n = 3 in Scheme 1).[33,34] In these oligomeric complexes, the oxo ligand of one molecule interacts with the sixth coordination site of a neighboring molecule, resulting in a $(V{=}O\cdots V{=}O)_n$ linear chain. The V=O stretching frequency is reduced to <900 cm^{-1} (relative to the normal 910−1035 cm^{-1}) due to donation of π-electrons from the strong V=O bond to the second metal center.

On the basis of the multiple structures of $V^{IV}O$(SALEN), it was anticipated that complex **1** would adopt a distorted square pyramidal geometry; this anticipation was proven correct by the X-ray crystal structure of complexes **1** (Figure 2). It was further anticipated that the increased space required by the additional methylene group (n = 3) would force one of the two imine nitrogens out of the basal plane of the distorted square pyramid, leading to a complex that was more trigonal bipyramidal. As is evidenced by the X-ray structure of complex **2**, only a modest distortion toward tbp geometry was achieved relative to complex **1**. (However, it is noted that the *tert*-butyl group was successful in preventing oligomer formation.) Since $\tau < 0.5$ for both of these complexes, they are best described as having distorted square pyramidal geometries. The V=O stretching frequencies for complexes **1** and **2** are 988 and 984 cm^{-1}, respectively, consistent with the terminal oxo ligand.

Since the two tetradentate ligands did not induce a significant tbp distortion, and due to our inability to prepare a pure complex with a butyl linker (n = 4 in Figure 1), sterically encumbered bidentate ligands were used. Vanadyl complexes of the type $V^{IV}OL_2$, where L is an N-substituted salicylaldimine derivative, have been studied extensively. Floriani and co-workers have structurally characterized the complex bis[*N*-(4-chlorophenyl)-salicylideneaminato]oxovanadium(IV) and found that it has a highly distorted square pyramidal geometry (τ = 0.43), suggesting that additional bulky substituents may increase the tbp nature of the molecular geometry.[20] Indeed, X-ray analysis of the bis-Schiff base complexes **3**−**5** confirms that the expected tbp vanadyl complexes can be readily prepared.

It is important to note the gross differences between the structures of complexes **1** and **2** (tetradentate ligands) and the structures of complexes **3**−**5** (bis-bidentate ligands). Even though both types of complexes have identical donor atoms consisting of two imine nitrogens and two phenolate oxygens, complexes **1** and **2** have oxygen trans to nitrogen, while in complexes **3**−**5** the two nitrogens are trans to each other as are the two phenolate oxygens. Thus, complexes **1** and **2** can have, at most, C_s symmetry (depending on the conformation of the N−N chelate ring), while complexes **3**−**5** can have, at most, C_2 symmetry. Interestingly, complex **3**, having minimal ligand bulk (N−Me, 6-H), is still best described as trigonal bipyramidal (τ = 0.55). This suggests an electronic preference for this distorted tbp geometry. Complex **4** is little changed from complex **3** despite the moderate increase in substituent size (N−*i*-Pr, 6-Me). Only upon adding the 6-*tert*-butyl substituent, as in complex **5**, is a dramatic increase in τ observed.

There are other examples in the literature of five-coordinate vanadyl compounds with nitrogen and/or oxygen donors that have $\tau > 0.50$. Dinuclear vanadyl tartrates can form trigonal bipyramidal structures about each vanadium atom. A *d*,*l* ligand combination forms a distorted square pyramidal geometry (τ values between 0.002 and 0.150),[35−42] while *d*,*d* and *l*,*l* ligand combinations yield distorted trigonal bipyramidal complexes (τ values from 0.59 to 0.65).[43,44] Bis(2-methyl-8-quinolinolato)-oxovanadium(IV) also has a distorted trigonal bipyramidal geometry with τ = 0.56.[16] For comparison, the vanadium(V)

(32) Collison, D.; Gahan, B.; Mabbs, F. E. *J. Chem. Soc., Dalton Trans.* **1987**, 111−117.
(33) Serrette, A.; Carroll, P. J.; Swager, T. M. *J. Am. Chem. Soc.* **1992**, *114*, 1887−1889.
(34) Kasahara, R.; Tsuchimoto, M.; Ohba, S.; Nakajima, K.; Ishida, H.; Kojima, M. *Inorg. Chem.* **1996**, *35*, 7661−7665.
(35) Garcia-Jaca, J.; Insausti, M.; Cortes, R.; Rojo, T.; Pizarro, J. L.; Arriortua, M. I. *Polyhedron* **1994**, *13*, 357−364.
(36) Garcia-Jaca, J.; Rojo, T.; Pizarro, J. L.; Goñi, A.; Arriortua, M. I. *J. Coord. Chem.* **1993**, *30*, 327−336.
(37) Wrobleski, J. T.; Thompson, M. R. *Inorg. Chem.* **1988**, *150*, 269−277.
(38) Beeson, H. D.; Tapscott, R. E.; Duesler, E. N. *Inorg. Chim. Acta* **1985**, *102*, 5−13.
(39) Ortega, R. B.; Tapscott, R. E.; Campana, C. F. *Inorg. Chem.* **1982**, *21*, 672−676.
(40) Hahs, S. K.; Ortega, R. B.; Tapscott, R. E.; Campana, C. F.; Morosin, B. *Inorg. Chem.* **1982**, *21*, 664−672.
(41) Ortega, R. B.; Campana, C. F.; Tapscott, R. E. *Acta Crystallogr.* **1980**, *B36*, 1786−1788.
(42) Tapscott, R. E.; Belford, R. L.; Paul, I. C. *Inorg. Chem.* **1968**, *7*, 356−364.
(43) Pizarro, J. L.; García-Jaca, J.; Rojo, T.; Arriortua, M. I. *Acta Crystallogr.* **1994**, *C50*, 1394−1396.
(44) Forrest, J. G.; Prout, C. K. *J. Chem. Soc. A* **1967**, 1312−1317.

Table 3. Transition Energies[a] and Extinction Coefficients (in Parentheses)[b] for Complexes **1**−**5** in CH_2Cl_2

assignment[c]	**1**	**2**	**3**	**4**	**5**
$\pi \rightarrow \pi^*$ or LMCT[d]	25 770 (7660)	25 840 (5980)	28 740 (5890)	28 250 (5100)	27 550 (4050)
$xy \rightarrow x^2 - y^2$ (band III)	16 000 (191)[e]	16 400 (154)	18 800 (62)	18 660 (71)	19 250 (95, sh)
$xy \rightarrow xz$ (band II)		14 290 (106, sh)[e]	16 900 (45)	16 720 (48, sh)	16 050 (49, sh)
$xy \rightarrow yz$ (band I)			12 000 (14)	11 980 (18)	11 760 (16)

[a] Energy in cm^{-1}. [b] In units of $cm^{-1}\ M^{-1}$. [c] For consistency, the labels are based on C_2 symmetry. For complexes **1** and **2** (C_s symmetry), switch xy and $x^2 - y^2$. [d] The $xy \rightarrow z^2$ transition is probably buried under this band. [e] Weak absorption tail to ≈9100 cm^{-1}.

Table 4. τ, EPR Parameters for Complexes **1**−**5** in Toluene at 150 K[a,b]

complex	τ	g_{xx}	g_{yy}	g_{zz}	$\lvert A_{xx}\rvert$[c] (10^{-4} cm^{-1})	$\lvert A_{yy}\rvert$[c] (10^{-4} cm^{-1})	$\lvert A_{zz}\rvert$[c] (10^{-4} cm^{-1})	$\lvert A_{xx} - A_{yy}\rvert$ (10^{-4} cm^{-1})
1	0.26	1.983	1.981	1.953	54.0	59.2	161.3	5.2
2	0.30	1.982	1.980	1.949	54.3	59.0	161.7	4.7
3	0.55	1.983	1.981	1.951	53.1	60.0	161.0	6.9
4	0.58	1.983	1.981	1.949	51.8	59.4	161.0	7.6
5	0.70	1.984	1.979	1.947	47.8	59.4	157.3	11.5

[a] Estimated error in $g = \pm 0.001$. [b] Estimated error in $A = \pm 0.5 \times 10^{-4}$ cm^{-1}. [c] Absolute values are reported since the sign of A cannot be directly determined from the EPR experiment.

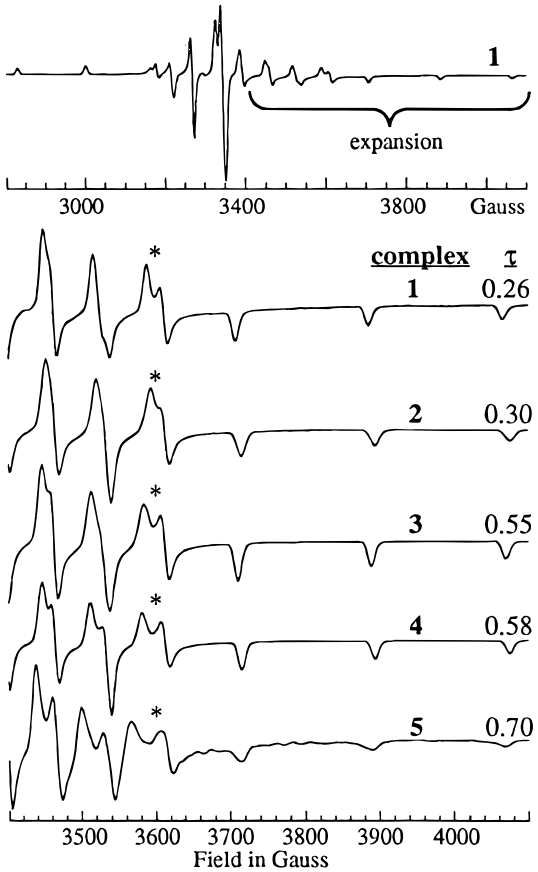

Figure 6. High-field region of the X-band EPR spectra of complexes **1**−**5** (in toluene at 150 K). The asterisk denotes region where rhombicity is most apparent.

complex recently reported by Carrano as a model for these trigonal bipyramidal vanadium−protein adducts has a τ-value of 0.37 or 0.67, depending on how one defines the α angle.[13]

The V═O stretching frequency is relatively insensitive to the square pyramidal-to-trigonal bipyramidal distortion. For complexes **1**−**5**, the V═O stretching frequencies are 988, 984, 980, 976, and 968 cm^{-1}, respectively, consistent with the terminal, not bridging, oxo ligand. Floriani has previously suggested that the low V═O stretching frequency (885 cm^{-1}) that was observed for bis[*N*-(4-chlorophenyl)salicylideneaminato)]oxovanadium-(IV) was due to the severely distorted square pyramidal geometry ($\tau = 0.43$).[20] This interpretation was later refuted by Hamilton who found that there were two crystalline forms of the complex, a needle form with ν(V═O) = 888 cm^{-1} and a prism form with ν(V═O) = 967 cm^{-1}, of which the needle form is probably a linear, oxo-bridged chain.[31] The data presented here for complexes **3**−**5** are in agreement with the interpretation of Hamilton and indicate that the energy of the V═O bond is only slightly sensitive to geometry (≈20 cm^{-1} for $\Delta\tau = 0.44$). The $V-O_{oxo}$ bond distance does not correlate directly with τ, considering that this distance is the same (within error) for complexes **4** and **5** while τ = 0.58 and 0.70, respectively.

The electronic spectra (Figure 5, Table 3) are typical of five-coordinate vanadyl complexes. Complexes **1** and **2** both have absorptions at ≈26 100 and ≈16 000 cm^{-1} with two shoulders to lower energy and absorption tailing out to <10 000 cm^{-1}. Complexes **3**−**5** each have a transition at approximately 28 000, 19 000, 16 500, and 12 000 cm^{-1}. The visible transitions are typically discussed in terms of the Ballhausen and Gray molecular orbital scheme (developed for $VO(SO_4)\cdot 5H_2O$, C_{4v} symmetry) in which the lowest energy transition (band I) is assigned as originating from promotion of an electron from the half-filled d_{xy} orbital to the empty d_{xz} or d_{yz} orbitals ($xy \rightarrow xz$, yz), and subsequent transitons as promotions from the half-filled d_{xy} orbital to the $d_{x^2-y^2}$ orbital (band II, $xy \rightarrow x^2 - y^2$) or the d_{z^2} orbital (band III, $xy \rightarrow z^2$).[45] Valek *et al.* have interpreted single-crystal polarized electronic spectroscopic studies on vanadyl bis-(acetylacetonate) ($VO(acac)_2$) in general agreement with the Ballhausen and Gray scheme (in C_{4v} nomenclature: $xy \rightarrow xz$, yz, ≈14 000 cm^{-1}; $xy \rightarrow x^2 - y^2$, ≈17 000 cm^{-1}; $xy \rightarrow z^2$, ≈25 000 cm^{-1}, with some uncertainty concerning the band III assignment).[46] In contrast, Collison and co-workers have assigned the low-energy (band I) transition of $VOX_2(tmu)_2$ (X = Cl, Br; tmu = tetramethylurea) as arising from promotion of an electron from the half-filled d_{xy} orbital to the $d_{x^2-y^2}$ ($xy \rightarrow x^2 - y^2$, ≈13 000 cm^{-1}) and subsequent transitons as promotions from the half-filled d_{xy} orbital to the d_{xz}, d_{yx} orbitals ($xy \rightarrow xz$, yz, ≈15 000 cm^{-1}) or the d_{z^2} orbital ($xy \rightarrow z^2$, ≈24 000 cm^{-1}).[47] For the complex $[VO(CN)_5]^{3-}$, the $xy \rightarrow x^2 - y^2$ transition occurs at ≈25 000 cm^{-1}. From this data it is evident that the energy of the $xy \rightarrow x^2 - y^2$ transition is, as expected, quite sensitive to the strength of the equatorial ligand field.

(45) Ballhausen, C. J.; Gray, H. B. *Inorg. Chem.* **1962**, *1*, 111−122.
(46) Valek, M. H.; Yeranos, W. A.; Basu, G.; Hon, P. K.; Belford, R. L. *J. Mol. Spectrosc.* **1971**, *37*, 229−239.
(47) Collison, D.; Gahan, B.; Garner, C. D.; Mabbs, F. E. *J. Chem. Soc., Dalton Trans.* **1980**, 667−674.

Through consideration of these single crystal electronic absorption studies, we have assigned the transitions of complexes **1**−**5** as indicated in Table 3, consistent with the orbital order $xy < yz < xz < x^2 - y^2 < z^2$. In the C_s symmetry of complexes **1** and **2**, and the C_2 symmetry of complexes **3**−**5**, the d_{xz} and d_{yz} orbitals are not degenerate, and therefore we can expect two transitions at low energy ($xy \rightarrow xz$ or yz). For complex **1**, these would be the absorptions making up the low-energy tail of the transtion centered at 16 000 cm^{-1}. For complex **2** these transitions make up the low-energy tail and the shoulder at 14 290 cm^{-1}. The transitions at 16 000 and 16 400 cm^{-1} in complexes **1** and **2**, respectively, are assigned to the $xy \rightarrow x^2 - y^2$ transition. For complexes **3**−**5**, the $xy \rightarrow xz$ and $xy \rightarrow yz$ transitions are assigned to the bands near 12 000 and 16 500 cm^{-1}. In complexes **3**−**5** the $xy \rightarrow x^2 - y^2$ transition is assigned to the absorption between 18 660 and 19 250 cm^{-1}. The peaks for complexes **1**−**5** at >26 000 cm^{-1} with large extinction coefficients probably include the $xy \rightarrow z^2$ transition and ligand associated (LMCT, $\pi \rightarrow \pi^*$) transitions. It is interesting to note that the $xy \rightarrow x^2 - y^2$ transitions of complexes **1** and **2** are at slightly lower energy than the corresponding band in $VO(acac)_2$, while the $xy \rightarrow x^2 - y^2$ transitions of complexes **3**−**5** are at slightly higher energy than the corresponding band in $VO(acac)_2$. This implies that the tetradentate ligands in complexes **1** and **2** provide a weaker ligand field than the acetylacetonate ligands of $VO(acac)_2$, while the bidentate Schiff base ligands of complexes **3**−**5** provide a stronger equatorial ligand field than the acetylacetonate ligands of $VO(acac)_2$.

The EPR spectra of complexes **1**−**5** are all rhombic with the rhombicity increasing with τ (as shown by $A_{xx} \neq A_{yy}$, Table 4). The coordinate system has been assigned by comparison of the g-values to those of bis(2-methyl-8-quinolinolato)oxovanadium(IV) (structurally similar to complexes **3**−**5**) for which a single-crystal EPR study has been reported.[32] The changing rhombicity in complexes **1**−**5** is easily seen in Figure 6 for the resonances marked with an asterisk. While A_{xx}, A_{yy}, and A_{zz} do not correlate with τ, the difference $|A_{xx} - A_{yy}|$ generally increases with τ. Complexes **1** and **2** are nearly axial with the difference $|A_{xx} - A_{yy}|$ being 5.2×10^{-4} and 4.7×10^{-4} cm^{-1}, respectively. Complexes **3** and **4** show intermediate rhombicity ($|A_{xx} - A_{yy}| = 6.9 \times 10^{-4}$ and 7.6×10^{-4} cm^{-1}, respectively), while complex **5** shows the largest rhombicity with $|A_{xx} - A_{yy}| = 11.6 \times 10^{-4}$ cm^{-1}.

A_{xx} is the most sensitive to variations in structure. A_{xx} varies from 54.3×10^{-4} to 47.8×10^{-4} cm^{-1} ($A_{xx,av} = (52.2 \pm 2.6) \times 10^{-4}$ cm^{-1}, error expressed as standard deviation), while A_{yy} varies from 60.0×10^{-4} to 59.0×10^{-4} cm^{-1} ($A_{yy,av} = (59.4 \pm 0.4) \times 10^{-4}$ cm^{-1}). The sensitivity of A_{xx} is intuitively appealing since the structure changes most along the molecular *x*-axis.

The relationships between the spin Hamiltonian parameters (g and A) and the electronic structure of d^1 complexes in various symmetries have been described nicely by Mabbs and Collison.[48] These relationships are shown in eqs 1 and 2, where ξ is the

$$g_{ij} = 2.0023\delta_{ij} - 2\xi\Lambda_{ij} \quad (1)$$

$$A_{ij} = P[-\kappa\delta_{ij} - 3c\mathbf{l}_{ij} - 2\xi\Lambda_{ij} + 3c\xi\Lambda'_{ij}] \quad (2)$$

one electron spin-orbit coupling constant for vanadium(IV) and δ_{ij} is the Kronecker delta. The terms Λ_{ij} and Λ'_{ij} mix excited state orbital angular momentum into the ground state. These terms depend on the d-orbital mixing coefficients for each excited state, and $1/\Delta E$ is the inverse of the energy difference between the ground state and excited state. The term $3c\mathbf{l}_{ij}$ is dependent only on the ground state and is the same for A_{xx} and A_{yy}. κ is the Fermi (isotropic) contact parameter and $P = g_e\beta_e g_N\beta_N\langle r^{-3}\rangle$ ($\langle r^{-3}\rangle$ is the inverse cube of the average nucleus-to-unpaired electron distance).

Considering only complexes **3**−**5** which are anticipated to have C_2 symmetry in solution and frozen solution, it is seen in Table 4 that g_{xx} and g_{yy} are insensitive (within error) to changes in structure. Thus, the changes in geometry have very little influence on the Λ_{ij} in eq 1. Accordingly, A_{xx} and A_{yy} are only slightly influenced by changes in structure as manifested in $-2\xi\Lambda_{ij}$ (eq 2). Since $g_{ij} - 2.0023 = -2\xi\Lambda_{ij}$ ($g_{ij} - 2.0023 = -0.023$ to -0.018 for $ij = xx$ or yy), the contribution of this term to A_{xx} and A_{yy} is $\approx -2.8 \times 10^{-4}$ to -2.2×10^{-4} cm^{-1} (assuming $P = 120 \times 10^{-4}$ cm^{-1}). Therefore, the slight decrease in A_{xx} observed as τ increases must be predominantly due to the effects of Λ'_{ij}. The difference $|A_{xx} - A_{yy}|$ is related to Λ_{ij} and Λ'_{ij} as shown in eq 3. This difference must also be

$$|A_{xx} - A_{yy}| = P[-2\xi\Lambda_{xx} - (-2\xi\Lambda_{yy}) + 3c\xi(\Lambda'_{xx} - \Lambda'_{yy})]$$
$$= P[g_{xx} - g_{yy} + 3c\xi(\Lambda'_{xx} - \Lambda'_{yy})] \quad (3)$$

due, in large part, to the Λ'_{ij} terms since $P(g_{xx} - g_{yy})$ is small for complexes **3**−**5** (0.6×10^{-4} cm^{-1} for complex **5**) compared to $|A_{xx} - A_{yy}|$ (11.6×10^{-4} cm^{-1} for complex **5**). As yet, we have not developed a bonding scheme that consolidates the observed EPR and UV−vis spectral results with this dependence of A on Λ'_{ij}. Studies in this area are ongoing.

It has been known for some time that the parallel component of the hyperfine coupling constant, A_{zz}, is sensitive to the donor type in the "equatorial" coordination sphere. From this knowledge, the empirical additivity relationship in eq 4 has been

$$A_{zz,calc} = \sum_i n_i A_{z,i} \quad (4)$$

developed as a means of determining, to a first approximation, the identity of the equatorial ligands in vanadyl complexes.[49] Here, n_i is the number of equatorial ligands of type i, and $A_{z,i}$ is the empirically determined contribution from each equatorial ligand of type i. The estimated error for eq 4 is $\pm 3 \times 10^{-4}$ cm^{-1}. While A_0, A_{xx}, A_{yy}, or A_{zz} can be used in eq 4, A_{zz} is most sensitive to the equatorial ligands. Additionally, A_{zz} can be determined with good accuracy directly from the spectral data without the need for computer simulation. Comparison of the calculated and experimental values of A_{zz} can be used to argue for or against the presence of specific ligands.[10,50−52]

The empirical parameters, $A_{z,i}$, in eq 4 have been determined for molecules of assumed square pyramidal geometry (or octahedral geometry with a weak sixth ligand).[49,50] An $A_{z,i}$ range of 31×10^{-4} (thiolate sulfur) to 46×10^{-4} cm^{-1} (water) is observed for biologically relevant ligands.[49] However, the applicability of eq 4 for structurally distorted molecules has never been addressed. Use of eq 4 and the values for $A_{z,i}$ in ref 49 gives $A_{zz,calc} = 159 \times 10^{-4}$ cm^{-1} for complexes **1**−**5**, which is very close to the experimental values for A_{zz} (Table 4). As

(48) Mabbs, F. E.; Collison, D. *Electron Paramagnetic Resonance of d Transition Metal Compounds*; Elsevier: Amsterdam, 1992; Vol. 16.
(49) Chasteen, N. D. In *Biological Magnetic Resonance*; Berliner, L. J., Reuben, J., Eds.; Plenum Press: New York, 1981; Vol. 3, pp 53−119.
(50) Cornman, C. R.; Zovinka, E. P.; Boyajian, Y. D.; Geiser-Bush, K. M.; Boyle, P. D.; Singh, P. *Inorg. Chem.* **1995**, *34*, 4213−4219.
(51) Houseman, A. L.; Morgan, L.; LoBrutto, R.; Frasch, W. D. *Biochemistry* **1994**, *33*, 4910−4917.
(52) Houseman, A. L. P.; LoBrutto, R.; Frasch, W. D. *Biochemistry* **1995**, *34*, 3277−3285.

the structure varies in complexes **3**−**5**, A_{zz} varies from 161.7 × 10^{-4} to 157.3 × 10^{-4} cm^{-1} ($A_{zz,av}$ = (160.5 ± 1.8) × 10^{-4} cm^{-1}). This small variation in A_z (≈2% of A_{zz}) suggests that eq 4 *also* holds for distorted molecules such as complex **5**, thereby supporting the continued use of eq 4 to make a first estimate of the equatorial ligands in vanadyl complexes.

To address the relative stability of complexes **3** and **5**, ethanol was added to toluene solutions of these complexes and EPR was used to estimate the amount of solvolysis. At 50% ethanol (by volume), complex **3** exhibited >25% solvolysis (as evidenced by a new set of parallel EPR transitions, data not shown), while complex **5** exhibited ≈10% solvolysis. This suggests that the more hindered coordination sphere around complex **5**, relative to complex **3**, precludes the ligand exchange reaction.

Conclusions

Vanadyl complexes can readily adopt distorted trigonal bipyramidal structures even with relatively minor steric crowding, as indicated by complexes **3** and **4**. Thus, vanadium in the +4 oxidation state is a suitable candidate as a transition state analogue for phosphoester hydrolysis, especially considering the inherent steric constraints of the active sites of protein tyrosine phosphatases. The V−O_{oxo} bond length and V═O stretching frequency are relatively insensitive to distortions along the sq pyr → tbp structural coordinate, implying that the low V═O stretching frequency (<900 cm^{-1}) observed for some vanadyl complexes is *not* due to a trigonal bipyramidal distortion away from the more common square pyramidal geometry. EPR spectroscopy is sensitive to these structural perturbations, as shown through the increase of $|A_{xx} - A_{yy}|$ with the increasing trigonal bipyramidal nature of the complex. The parallel coupling constant, A_{zz}, is relatively insensitive to these structural changes, indicating that the EPR additivity relationship is applicable to distorted complexes.

Acknowledgment. The insightful comments of the reviewers are gratefully acknowledged. The authors thank Professor B. Wang for the use of his UV−vis spectrometer and Professor M.-H. Whangbo for helpful discussions. Funding for this work was provided by the National Science Foundation NSF; (Grant CHE-9702873) and the Donors of the Petroleum Research Fund, administered by the American Chemical Society. The X-ray diffractometer was purchased using funds from the NSF (Grant CHE-9509532).

Supporting Information Available: Figures S1 and S2, showing EPR spectra and simulations for **1**−**5**, and Figures S3−S7, providing full numbering schemes for **1**−**5** (7 pages). Five X-ray crystallographic files, in CIF format, are available on the Internet. Ordering and access information is given on any current masthead page.

IC970868Z